Hazenite, KNaMg$_2$(PO$_4$)$_2$·14H$_2$O, a new biologically related phosphate mineral, from Mono Lake, California, U.S.A.

Hexiong Yang,[1,*] Henry J. Sun,[2] and Robert T. Downs[1]

[1]Department of Geosciences, University of Arizona, 1040 East 4th Street, Tucson, Arizona 85721, U.S.A.
[2]Desert Research Institute, 755 Flamingo Road, Las Vegas, Nevada 89119, U.S.A.

Abstract

A new biologically related, struvite-type phosphate mineral, hazenite, ideally KNaMg$_2$(PO$_4$)$_2$·14H$_2$O, has been found in and/or on completely dried-out or decomposed cyanobacteria on porous calcium-carbonate (mainly calcite and aragonite) substrates in Mono Lake, California. The mineral occurs as radiating clusters of prismatic crystals and is colorless, transparent with white streak and vitreous luster. It is brittle, with the Mohs hardness of 2~2.5; cleavage is good on {001} and no twinning was observed. The measured and calculated densities are 1.91(3) and 1.88(2) g/cm^3, respectively. Hazenite is biaxial (+), with n_α =1.494(1), n_β = 1.498(1), n_γ = 1.503(1), $2V_{meas}$ = 41(2)°, $2V_{calc}$ = 42°, $X = b$, $Y = c$, $Z = a$, and does not fluoresce under long- or short-wave ultraviolet rays. The dispersion is strong with $r < v$. It is soluble in water. The electron microprobe analysis yielded an empirical formula of K$_{0.97}$(Na$_{0.96}$Ca$_{0.02}$)Mg$_{2.07}$[(P$_{0.98}$S$_{0.02}$)O$_4$]$_2$·13.90H$_2$O. Hazenite is orthorhombic with space group $Pmnb$ and unit-cell parameters a = 6.9349(4) Å, b = 25.174(2) Å, c = 11.2195(8) Å, and V = 1958.7(3) Å^3. There are many structural similarities between hazenite and struvite, as also revealed by their Raman spectra. The hazenite structure contains six symmetrically independent non-hydrogen cation sites, two for Mg^{2+} (Mg1 and Mg2), two for P^{5+} (P1 and P2), one for Na$^+$, and one for K$^+$. It can be viewed as three types of layers stacking along the **b**-axis, in a repeating sequence of ABCBABCB…, where layer A consists of Mg1(H$_2$O)$_6$ octahedra and NaO$_6$ trigonal prisms, layer B of P1O$_4$ and P2O$_4$ tetrahedra, and layer C of Mg2(H$_2$O)$_6$ octahedra and very irregular KO$_6$ polyhedra. These layers are linked together by hydrogen bonds, plus the K-O bonds between layers B and C (K-O5-P2). Interestingly, the combination of layers B and C in hazenite exhibits a configuration analogous to the struvite-(K) structure. Hazenite is believed to form in high pH environments through the involvement of cyanobacterial activities. To our knowledge, hazenite is the first struvite-type compound that contains two structurally distinct monovalent cations (K and Na), pointing to an exclusive role of biological activity in the mineralization process.

Keywords: Hazenite, struvite-type materials, phosphates, biomineral, crystal structure, X-ray diffraction, Raman spectra

Introduction

A new biologically related, struvite-type phosphate mineral, hazenite, KNaMg$_2$(PO$_4$)$_2$·14H$_2$O, has been found on the shoreline of Mono Lake, California. Mono Lake, located in the hydrologically closed Mono basin, eastern California, U.S.A., is known for its outstanding biological and geochemical features (Wiens et al. 1993 and references therein). This terminal lake currently consists of a hypersaline (84–92 g/L), alkaline (pH = 9.8) Na-CO$_3$-Cl-SO$_4$ brine, resulting from evaporative concentration of inflow water, rock weathering, and mineral precipitation (e.g., Garrels and Mackenzie 1967; Li et al. 1997; Oremland et al. 2004). The lake is endorheic and the basin's volcanic setting includes numerous hydrothermal springs that contribute to its unique water chemistry (Bischoff et al. 1991; Council and Bennett 1993; Budinoff and Hollibaugh 2007). High concentrations of boron (~34 mmol/L) and minor amounts of K, Mg, and Ca are

found in the lake (e.g., Bischoff et al. 1991). Dissolved organic carbon concentration is ~6.7 mmol/L (Melack 1983), and phosphate is as high as 1.0 mmol/L (Mono Basin Ecosystem Study Committee 1987). The food web of Mono Lake is relatively simple, consisting of bacteria, phytoplankton, brine flies *Ephedra hians*, the brine shrimp *Artemia monica*, and migrating and nesting birds (Jørgensen et al. 2008 and references therein). Soda lakes, such as Mono Lake, are good analogs of putative ancient Martian and Archaean terrestrial aquatic biomes and represent environmental extremes in terms of their high pH and salinities. They can also be sensitive indicators of local climate changes and provide records of paleoclimate (Stine 1994; Jellison et al. 1996; Benson et al. 1998; Hollibaugh et al. 2001). Nevertheless, Mono Lake is subject to recurrent periods of meromixis (persistent chemical stratification) as a consequence of natural and anthropogenic alterations of freshwater flow into the lake, with the most recent episodes persisting from 1995 until 2003, and from 2005 until 2007 (Budinoff and Hollibaugh 2007).

Several unusual biologically related phosphate miner-

* E-mail: hyang@u.arizona.edu

als have been found from Mono Lake, including newberyite $MgHPO_4 \cdot 3H_2O$ (Cohen and Ribbe 1966; Ribbe and Cohen 1966), monetite $CaHPO_4$ (Cohen and Ribbe 1966; Ribbe and Cohen 1966), struvite $(NH_4)MgPO_4 \cdot 6H_2O$ (Cooper and Dunning 1969), and possibly brushite $CaHPO_4 \cdot 2H_2O$ (Walker 1988). In addition, ikaite, $CaCO_3 \cdot 6H_2O$, not previously observed in lake environments, precipitates seasonally along the shore of Mono Lake (Shearman et al. 1989; Council and Bennett 1993; Bischoff et al. 1993). Another relatively rare mineral gaylussite, $Na_2Ca(CO_3)_2 \cdot 5H_2O$, was also found in Mono Lake, which is believed to presently precipitate in a year-round process that probably only began after 1970 when the salinity of the lake exceeded 80‰ (Bischoff et al. 1991), owing to the diversion of tributary streams by the Los Angeles Department of Water and Power. The salinity of Mono Lake has steadily increased since 1941 from 50‰ to the current ~90‰ (Bischoff et al. 1991; Budinoff and Hollibaugh 2007; Jørgensen et al. 2008). In this paper, we report a new biologically related phosphate mineral, hazenite $KNaMg_2(PO_4)_2 \cdot 14H_2O$, discovered at this locality. The new mineral is named after Robert Miller Hazen, a staff scientist at the Geophysical Laboratory, Carnegie Institution of Washington, for his outstanding contributions to Earth sciences in general, and mineralogy in particular, in both research and education, as well as for his contributions to understanding interactions between minerals and organic molecules. Part of the cotype sample has been deposited at the Mineral Museum of the University of Arizona (Catalog no. 18812). The new mineral and its name have been approved by the Commission on New Minerals and Nomenclature and Classification (CNMNC) of the International Mineralogical Association (IMA2007-061).

SAMPLE DESCRIPTION AND EXPERIMENTAL METHODS

Occurrence, physical, and chemical properties, and Raman spectra

Hazenite was found in and/or on completely dried-out or decomposed green algae (cyanobacteria) on porous calcium-carbonate (mainly calcite and aragonite) substrates or tufas on the south shore of Mono Lake (lat. 37°56′31″N, long. 119°1′42″W). It is observed as radiating clusters or tufts of elongated (along [100]) prismatic crystals up to $0.40 \times 0.12 \times 0.06$ mm (Fig. 1). The mineral is colorless, transparent with white streak and vitreous luster. It is brittle, with Mohs hardness of 2~2.5; cleavage is good on {001} and no twinning was observed. The measured

FIGURE 1. Photograph of hazenite crystals.

and calculated densities are 1.91(3) and 1.88(2) g/cm³, respectively. Hazenite decomposes easily in 10% HCl at room temperature and dissolves slowly in water. Optically, it is biaxial (+), with $n_\alpha = 1.494(1)$, $n_\beta = 1.498(1)$, $n_\gamma = 1.503(1)$, $2V_{meas} = 41(2)°$, $2V_{calc} = 42°$, $X = b$, $Y = c$, $Z = a$, and does not fluoresce under long- or short-wave ultraviolet light. The dispersion is strong with $r < v$.

The chemical composition was determined with a CAMECA SX50 electron microprobe at 10 kV and 5 nA (http://rruff.info), yielding an average composition (wt%) (20 points) of K_2O 8.27(28), Na_2O 5.35(26), MgO 15.09(41), CaO 0.21(26), P_2O_5 25.27(43), SO_3 0.54(50), and H_2O (by difference, to sum up to 100%) 45.27. Based on the number of oxygen atoms bonded to P^{5+}, which is 8 (see below), we obtain an empirical formula of $K_{0.97}(Na_{0.96}Ca_{0.02})Mg_{2.07}[(P_{0.98}S_{0.02})O_4]_2 \cdot 13.90H_2O$, which can be simplified ideally as $KNaMg_2(PO_4)_2 \cdot 14H_2O$.

The Raman spectra of hazenite were collected on a randomly oriented crystal from 9 scans at 30 s and 100% power per scan on a Thermo Almega microRaman system, using a solid-state laser with a wavelength of 532 nm and a thermoelectricaly cooled CCD detector. The laser is partially polarized with 4 cm⁻¹ resolution and a spot size of 1 μm.

X-ray crystallography

Both powder and single-crystal X-ray diffraction data of hazenite were collected on a Bruker X8 APEX2 CCD X-ray diffractometer equipped with graphite-monochromatized Mo$K\alpha$ radiation. Based on orthorhombic symmetry (see below), the unit-cell parameters determined from the powder X-ray diffraction data (Table 1)

TABLE 1. Powder X-ray diffraction data for hazenite

Intensity	d_{meas}	d_{calc}	h k l
6	5.899(5)	5.903	1 0 1
17	5.606(6)	5.600	0 0 2
11	5.485(5)	5.480	0 4 1
4	5.120(3)	5.123	0 2 2
7	4.824(3)	4.827	1 3 1
30	4.659(3)	4.656	1 4 0
100	4.302(5)	4.298	1 4 1
22	4.184(9)	4.175	0 4 2
11	3.744(1)	3.744	0 5 2
3	3.468(8)	3.460	2 0 0
20	3.262(6)	3.268	1 1 3
6	3.081(3)	3.078	2 3 1
6	3.027(9)	3.037	0 8 1
11	2.931(1)	2.930	2 4 1
32	2.803(3)	2.805	0 0 4
43	2.786(5)	2.790	0 1 4
51	2.767(2)	2.766	2 5 1
48	2.742(1)	2.743	0 8 2
51	2.670(1)	2.671	2 4 2
2	2.560(4)	2.556	0 4 4
3	2.529(2)	2.531	2 1 3
7	2.357(1)	2.358	2 4 3
6	2.329(3)	2.327	2 8 0
4	2.209(1)	2.210	1 6 4
9	2.180(3)	2.177	2 0 4
10	2.172(1)	2.172	2 1 4
10	2.151(1)	2.151	2 8 2
11	2.075(3)	2.074	2 7 3
6	2.000(2)	2.003	2 5 4
3	1.914(6)	1.908	3 3 3
8	1.882(1)	1.883	2 1 11
7	1.881(6)	1.874	2 9 3
7	1.831(1)	1.830	3 5 3
7	1.804(2)	1.802	2 4 5
7	1.794(1)	1.793	2 1 20
7	1.749(1)	1.748	0 9 5
5	1.745(1)	1.744	3 3 4
11	1.734(1)	1.733	4 0 0
5	1.709(2)	1.711	2 1 22
3	1.667(2)	1.666	3 8 3
4	1.614(1)	1.614	2 3 6
2	1.591(1)	1.590	2 4 6
2	1.466(1)	1.466	4 8 2
2	1.371(2)	1.373	4 9 3
2	1.355(1)	1.355	5 4 0
3	1.345(1)	1.345	5 4 1
2	1.319(2)	1.321	3 8 6
3	1.291(1)	1.291	3 1 61
2	1.258(1)	1.258	2 5 8

are $a = 6.936$ (2), $b = 25.15$ (1), $c = 11.212$ (4) Å, and $V = 1956$ (1) Å³. For comparison, included in Table 1 are also the powder X-ray diffraction data calculated using the program XPOW (Downs et al. 1993) based on the determined structure.

Single-crystal X-ray diffraction data of hazenite were collected from a nearly equi-dimensional crystal ($0.05 \times 0.05 \times 0.06$ mm) with frame widths of 0.5° in ω and 30 s counting time per frame. All reflections were indexed on the basis of an orthorhombic unit-cell (Table 2). The intensity data were corrected for X-ray absorption using the Bruker program SADABS. The systematic absences of reflections suggest possible space group $Pmnb$ (62) or $P2_1nb$ (33). The crystal structure was solved and refined using SHELX97 (Sheldrick 2008) based on the space group $Pmnb$, because it yielded the better refinement statistics in terms of bond lengths and angles, atomic displacement parameters, and R factors. The detailed structure refinement procedures were similar to those described by Yang and Sun (2004). The positions of all atoms were refined with anisotropic displacement parameters,

except for H atoms, which were refined with a fixed isotropic displacement parameter ($U_{eq} = 0.04$). Final coordinates and displacement parameters of atoms are listed in Table 3, and selected bond distances in Table 4.

DISCUSSION

Crystal structure

The structure of hazenite is identical to that of the bacteria-formed phosphate reported by Yang and Sun (2004), who have given a detailed structural description of this compound, including its hydrogen bonding and structural relationships with struvite-type materials. However, for a direct comparison with struvite-type materials, we have adapted a different unit-cell setting for hazenite (Table 5). Specifically, the a and b axes for the phosphate compound studied by Yang and Sun (2004) are

TABLE 2. Summary of crystallographic data and refinement results for hazenite from single-crystal X-ray diffraction

Ideal structural formula	KNaMg₂(PO₄)₂·14H₂O
Space group	$Pmnb$ (no. 62)
a (Å)	6.9349(4)
b (Å)	25.1737(15)
c (Å)	11.2195(8)
V (Å³)	1958.7(3)
Z	4
ρ_{calc} (g/cm³)	1.875
λ (Å)	0.71069
μ (mm⁻¹)	0.62
θ range for data collection	1.62 to 28.11
No. of reflections collected	11511
No. of independent reflections	2416
No. of reflections with $I > 2\sigma(I)$	2339
No. of parameters refined	198
R_{int}	0.035
Final R factors [$I > 2\sigma(I)$]	$R1 = 0.042$, $wR2 = 0.090$
Final R factors (all data)	$R1 = 0.045$, $wR2 = 0.093$
Goodness-of-fit	1.21

TABLE 4. Selected non-hydrogen bond distances (Å) in hazenite

P1-O1	1.544(3)	P2-O4	1.535(3)
P1-O2	1.540(3)	P2-O5	1.534(3)
P1-O3 (×2)	1.530(2)	P2-O6 (×2)	1.543(2)
Avg.	1.536	Avg.	1.539
Mg1-OW7	2.032(3)	Mg2-OW11 (×2)	2.060(2)
Mg1-OW8	2.040(3)	Mg2-OW12 (×2)	2.074(2)
Mg1-OW9 (×2)	2.066(2)	Mg2-OW13	2.093(3)
Mg1-OW10 (×2)	2.083(2)	Mg2-OW14	2.109(3)
Avg.	2.062	Avg.	2.078
K-O5	2.672(3)	Na-OW10 (×2)	2.563(3)
K-OW11 (×2)	2.980(2)	Na-OW15 (×2)	2.425(3)
K-OW12 (×2)	2.908(2)	Na-OW15 (×2)	2.472(3)
K-OW13	3.064(3)		
Avg.	2.919	Avg.	2.487

TABLE 3. Coordinates and displacement parameters of atoms for hazenite

Atom	x	y	z	U_{11} (Å²)	U_{22} (Å²)	U_{33} (Å²)	U_{23} (Å²)	U_{13} (Å²)	U_{12} (Å²)	U_{eq} (Å²)
K	3/4	0.2216(1)	0.5014(1)	0.0535(7)	0.0290(6)	0.0376(6)	−0.0096(4)	0	0	0.0401(4)
Na	3/4	0.0004(1)	0.9259(2)	0.0272(10)	0.0405(11)	0.0384(11)	0.0091(8)	0	0	0.0354(6)
Mg1	3/4	0.9543(1)	0.6388(1)	0.0140(7)	0.0149(6)	0.0175(6)	0.0022(4)	0	0	0.0155(4)
Mg2	3/4	0.2237(1)	0.8366(1)	0.0185(7)	0.0154(6)	0.0169(7)	0.0004(4)	0	0	0.0169(4)
P1	1/4	0.1281(1)	0.7219(1)	0.0143(5)	0.0127(5)	0.0145(5)	0.0001(3)	0	0	0.0138(3)
P2	3/4	0.1272(1)	0.2201(1)	0.0113(5)	0.0129(5)	0.0152(5)	0.0023(3)	0	0	0.0131(3)
O1	1/4	0.1358(1)	0.8584(2)	0.0256(14)	0.0311(14)	0.0225(13)	−0.0032(11)	0	0	0.0264(6)
O2	1/4	0.1828(1)	0.6608(2)	0.0287(14)	0.0159(12)	0.0277(14)	0.0033(10)	0	0	0.0241(6)
O3	0.4317(3)	0.0976(1)	0.6859(2)	0.0184(9)	0.0218(9)	0.0267(9)	−0.0006(7)	−0.0006(7)	0.0012(7)	0.0223(4)
O4	3/4	0.0673(1)	0.1945(3)	0.0229(13)	0.0157(12)	0.0357(15)	−0.0027(10)	0	0	0.0248(6)
O5	3/4	0.1380(1)	0.3546(2)	0.0223(13)	0.0258(13)	0.0172(12)	0.0001(10)	0	0	0.0217(6)
O6	0.9315(3)	0.1519(1)	0.1630(2)	0.0156(9)	0.0256(9)	0.0227(9)	0.0047(7)	0.0026(7)	−0.0021(7)	0.0213(4)
OW7	3/4	0.0095(1)	0.5068(3)	0.0214(14)	0.0303(16)	0.0410(17)	0.0174(13)	0	0	0.0309(7)
OW8	3/4	0.8944(1)	0.7614(3)	0.0138(13)	0.0440(18)	0.0510(19)	0.0293(15)	0	0	0.0363(8)
OW9	0.5349(3)	0.9161(1)	0.5446(2)	0.0220(10)	0.0333(10)	0.0211(9)	−0.0016(7)	0.0024(8)	−0.0094(8)	0.0255(4)
OW10	0.9578(3)	0.9947(1)	0.7375(2)	0.0208(10)	0.0192(9)	0.0333(10)	0.0005(8)	−0.0049(8)	−0.0017(8)	0.0244(4)
OW11	0.5359(3)	0.2493(1)	0.7231(2)	0.0301(12)	0.0212(1)	0.0412(12)	0.0051(8)	−0.0117(9)	0.0002(8)	0.0308(5)
OW12	0.9662(3)	0.1966(1)	0.9489(2)	0.0281(11)	0.0297(10)	0.0215(9)	0.0038(8)	0.0006(8)	0.0040(8)	0.0264(5)
OW13	3/4	0.1554(1)	0.7305(3)	0.0203(14)	0.0229(14)	0.0479(18)	−0.0114(12)	0	0	0.0304(7)
OW14	3/4	0.2975(1)	0.9256(3)	0.0768(25)	0.0176(14)	0.0270(16)	−0.0042(11)	0	0	0.0405(8)
OW15	0.0100(3)	0.0597(1)	0.9823(2)	0.0404(13)	0.0301(11)	0.0326(11)	−0.0035(8)	0.0081(10)	0.0002(9)	0.0344(5)
H11	0.841(5)	0.026(1)	0.484(3)							
H21	0.850(5)	0.879(1)	0.790(3)							
H31	0.454(5)	0.896(1)	0.572(3)							
H32	0.549(5)	0.909(1)	0.467(3)							
H41	0.057(6)	0.977(1)	0.758(3)							
H42	0.999(5)	0.023(2)	0.723(3)							
H51	0.450(6)	0.230(1)	0.707(3)							
H52	0.503(5)	0.278(2)	0.714(3)							
H61	0.940(5)	0.181(1)	0.017(3)							
H62	0.051(6)	0.179(1)	0.921(3)							
H71	0.847(5)	0.135(1)	0.722(3)							
H81	3/4	0.327(2)	0.890(5)							
H82	3/4	0.305(2)	0.003(5)							
H91	0.057(6)	0.080(1)	0.946(3)							
H92	0.954(5)	0.076(1)	0.039(3)							

TABLE 5. Comparison of crystallographic data for hazenite and other struvite-type materials

Chemical formula	Struvite $(NH_4)Mg(PO_4)\cdot 6H_2O$	Struvite-(K) $KMg(PO_4)\cdot 6H_2O$	Synthetic $NaMg(PO_4)\cdot 7H_2O$	Hazenite $KNaMg_2(PO_4)_2\cdot 14H_2O$
a (Å)	6.955(1)	6.903	6.731(2)	6.9349(4)
b (Å)	6.142(1)	6.174	6.731(2)	25.1737(15)
c (Å)	11.218(2)	11.164	10.982(4)	11.2195(8)
V (Å³)	479.2	475.03	497.5	1958.7
Space group	$Pmn2_1$ (no. 31)	$Pmn2_1$ (no. 31)	$P4_2/mmc$ (no. 131)	$Pmnb$ (no. 62)
Z	2	2	2	4
ρcal (g/cm³)	1.71	1.88	1.77	1.88
Strong powder lines	4.257(100)	4.26(100)	2.869(100)	4.302(100)
	5.601(60)	3.27(90)	5.739(98)	2.767(50)
	2.919(55)	4.14(80)	4.255(91)	2.670(50)
	2.690(50)	2.650(70)	6.731(66)	2.742(50)
	2.660(45)	2.699(50)	2.380(56)	2.786(40)
	5.905(40)	2.905(50)	1.798(45)	2.803(30)
	4.139(40)		3.366(40)	4.659(30)
Reference	1	2	3	4

Note: References: 1 = Ferraris et al. (1986); 2 = Graeser et al. (2007); 3 = Mathew et al. (1982); 4 = This study.

switched in hazenite.

There are many structural similarities between hazenite and struvite-type materials, which have been of great interest because of their broad and important biological, agricultural, and industrial implications (e.g., Dickens and Brown 1972; Banks et al. 1975; Angoni et al. 1998; Doyle and Parsons 2002; Trobajo et al. 2007; Haferburg et al. 2008; Weil 2008; Chen et al. 2010). For example, Mg^{2+} cations in these compounds are all coordinated octahedrally by six H_2O molecules whose H atoms are strongly bonded to oxygen atoms in $(PO_4)^{3-}$ groups. No H_2O molecules are shared between $Mg(H_2O)_6$ octahedra. Excluding H^+, there are six symmetrically nonequivalent cation sites in hazenite, two for Mg^{2+} (Mg1 and Mg2), two for

P^{5+} (P1 and P2), one for Na^+, and one for K^+. Viewed along **c**, the hazenite structure can be considered as stacking of three types of layers along the **b**-axis, in a repeating sequence of ABCBABCB… (Fig. 2a), where layer A consists of $Mg1(H_2O)_6$ octahedra and NaO_6 trigonal prisms, layer B of $P1O_4$ and $P2O_4$ tetrahedra, and layer C of $Mg2(H_2O)_6$ octahedra and very irregular KO_6 polyhedra. These layers are linked together by hydrogen bonds, plus the K-O bonds between layers B and C (K-O5-P2). Interestingly, the combination of layers B and C in hazenite exhibits a configuration directly comparable with the struvite-(K) structure (Mathew and Schroeder 1979; Graeser et al. 2008) (Fig. 2b). In fact, the struvite-(K) structure can be readily achieved from the hazenite structure with a


(a) Hazenite

(b) Struvite-(K)
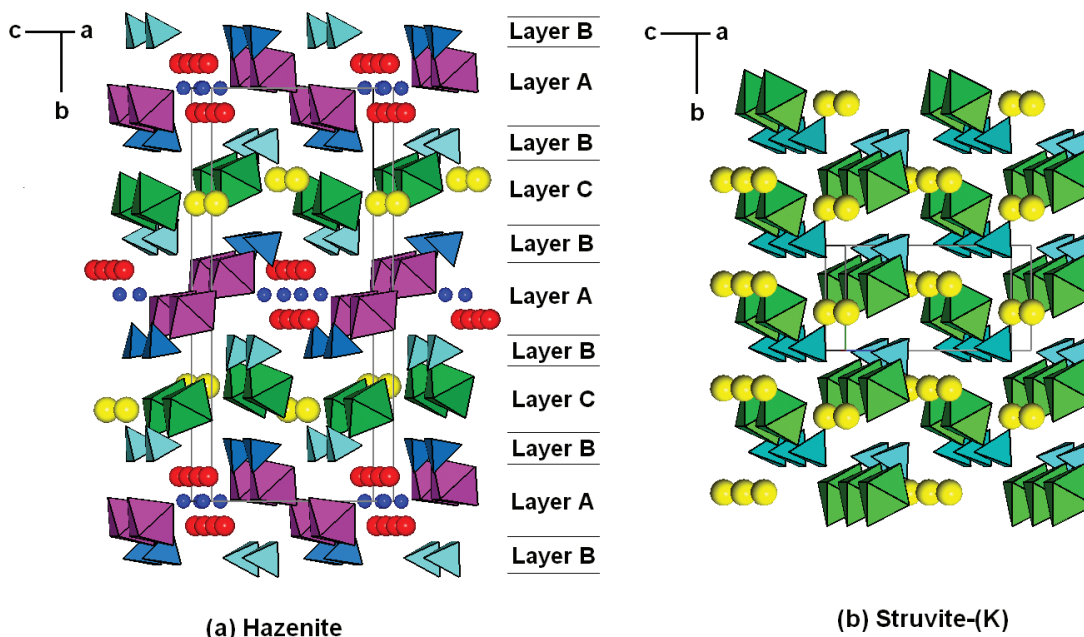
FIGURE 2. (**a**) Crystal structure of hazenite. Tetrahedra = PO_4^{3-} groups and octahedra = $Mg(H_2O)_6$. The largest, medium, and smallest spheres represent K, Ow9 (the water molecule bonded to Na only), and Na, respectively. See the text for the definition of layers A, B, and C. (**b**) Crystal structure of struvite-(K). Tetrahedra, octahedra, and spheres represent PO_4^{3-} groups, $Mg(H_2O)_6$, and K, respectively.

substitution of layer C for layer A, although the average K-O bond length (2.919 Å) in hazenite is slightly shorter than that (3.034 Å) in struvite-(K). However, the combination of layers A and B in hazenite does not show much resemblance to the $NaMgPO_4 \cdot 7H_2O$ structure determined by Mathew et al. (1982). In particular, as noted by Yang and Sun (2004), Na^+ in hazenite is situated in a six-coordinated trigonal prism, with four H_2O molecules bonded to Na^+ cations only, and each prism shares two edges with two neighboring prisms to form zigzag chains parallel to **a**, accounting for its elongated morphology along [100]. In contrast, Na^+ in $NaMgPO_4 \cdot 7H_2O$ is in an elongated octahedron, with two H_2O molecules bonded to Na^+ only, and each octahedron sharing two corners with two other $Na(H_2O)_6$ octahedra to form straight chains along **c**.

Dickens and Brown (1972) examined several struvite-type compounds and their structural relationships and presented a general chemical formula for such materials: $M^+X^{2+}(YO_4) \cdot nH_2O$, where $n = 6$–8, Y = P or As, and the radius of monovalent M^+ is greater than that of divalent X^{2+}. Banks et al. (1975) and Weil (2008) investigated several struvite analogs of the type $M^+MgYO_4 \cdot 6H_2O$ ($M^+ = NH_4$, K, Rb, Cs, and Tl). Recently, struvite analogs with X^{2+} = Co and Ni have been reported (Blachnik et al. 1997; Touaiher et al. 2001; El Bali et al. 2005; Trobajo et al. 2007; Haferburg et al. 2008). Although Na^+ ions have been included in many laboratory synthesis preparations, no Na-analog of the struvite-type structure has been identified thus far (e.g., Banks et al. 1975; Mathew et al. 1982). It therefore has been generally agreed that the struvite-type structure is unable to accommodate monovalent M^+ cations smaller than K^+ and the incorporation of Na^+ requires extra H_2O molecules ($n > 6$) to compensate its smaller ionic size, as in $NaMgPO_4 \cdot 7H_2O$ (Mathew et al. 1982) and $NaNiPO_4 \cdot 7H_2O$ (Trobajo et al. 2007). Clearly, the determination of the hazenite structure provides further support to this statement. Furthermore, to our knowledge, hazenite is the first struvite-type compound that contains two structurally distinct M^+ cations (K and Na), pointing to the exclusive role of biological activities in its mineralization process.

Raman spectra

There have been numerous studies on struvite-related materials by means of infrared and Raman spectroscopic techniques (Banks et al. 1975; Angoni et al. 1998; Stefov et al. 2004, 2005; Frost et al. 2005; Koleva 2007). Yang and Sun (2004) measured the infrared spectrum of hazenite and showed the remarkable similarities in the IR spectra between hazenite and struvite. Here, we present our Raman spectroscopic measurements of hazenite in Figure 3, along with the Raman spectra of a struvite sample from the RRUFF project (deposition R050540: http://rruff.info/R050540) for comparison. A tentative assignment of major Raman bands for hazenite is given in Table 6. It is evident from Figure 3 that the PO_4 symmetric stretching (v_1) mode at ~934 cm^{-1} for hazenite is shifted to lower frequency relative to that for struvite by ~13 cm^{-1}. This shift is expected, because, as compared with the NH_4^+-O bonds in struvite, the stronger M^+ (=K, Na)-O interactions in hazenite make the intra-molecular P-O bonds weaker, giving rise to the shift of the P-O stretching mode to lower frequency. Similar observations have been reported for struvite-type compounds by Stefov et al. (2004, 2005) and for
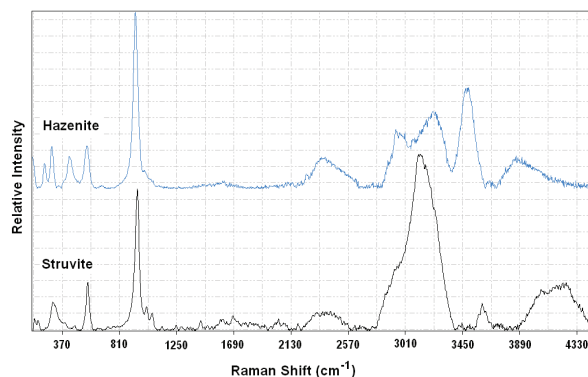
FIGURE 3. Raman spectrum of hazenite, along with that of struvite taken from the RRUFF project (see the text for details) for comparison. The spectra are shown with vertical offset for more clarity.

TABLE 6. Tentative assignment of Raman bands for hazenite

Bands (cm^{-1})	Intensity	Assignment
3900–2500	Relatively strong, broad	Water v_1-v_3 sym- and antisymmetric stretching
2380	Weak, broad	Water-phosphate hydrogen bonding
1620	Very weak, broad	Water bending
1100–988	Shoulder, week	v_3 (PO_4) antisymmetric stretching
935	Strong, sharp	v_1 (PO_4) symmetric stretching
685	Very weak	Water-water H bonding
565	Relatively strong, sharp	v_4 (PO_4) antisymmetric bending
430	Relatively strong, sharp	v_2 (PO_4) symmetric bending
290	Relatively strong, sharp	Mg-O stretching
258–136	Relatively strong, multi-peaks	Lattice and Mg-O vibrational modes

dittmarite-type compounds $M'M''PO_4 \cdot H_2O$ (M' = K^+, NH_4^+; M'' = Mn^{2+}, Co^{2+}, Ni^{2+}) by Koleva (2007).

Formation

Hazenite was first found to form in a microbiological culture containing the filamentous, photosynthetic cyanobacterium *Lyngbya sp.*, which was isolated from the interior of calcareous tufa deposits collected from Mono Lake (Yang and Sun 2004). The growth medium was composed of distilled water and the lake water in an 1:1 ratio, solidified with 1.2% agar. At the end of growth and as the medium in the petri dish dried up, a few tufts of elongated-tabular crystals of hazenite appeared around dead cyanobacterial colonies. Following this discovery, the subsequent field trips to Mono Lake led us to find the mineral in nature.

Struvite is a relatively rare mineral in nature and its formation by microorganisms was first documented as early as in the 19th century (Robinson 1889). It is well known now that struvite can form inside living bacteria, as a diagenetic byproduct of bird feces, in kidney stones, or in association with decaying organisms or decomposing organic matter (such as in old graveyards, under floors of stables, in guano, or wastewater treatments). One common feature shared by these environments is high alkalinity, suggesting that high pH conditions are necessary for the formation of struvite and/or similar phosphate minerals (Rivadeneyra et al. 1993; Grover et al. 1997; Doyle and Parsons 2002; Chen et al. 2010). Because of the very hypersalinity and high alkalinity of the Mono Lake water, hazenite is also believed to form in high-pH conditions with the strong involvement of cyanobacte-

rial activities. Yang and Sun (2004) suggested that phosphate metabolism or phosphate-containing organic compounds could be a good source for inorganic phosphate. In the cytoplasm of a living bacterium, much of the phosphate in a cell occurs in the form of phospholipids in the membranes. Presumably, following the death of algae, the slow breakdown of phosphorus-containing organic compounds, on the one hand, would become the steady supply for phosphate. The lake water, on the other hand, provides Na, K, and Mg for the hazenite formation. In addition, the cell membranes may be energetically favored for nucleation of crystals, as they can provide structures that serve as substrates for heterogeneous crystal nucleation (with lower energy barrier than homogeneous nucleation) and stereochemical arrangements for the mineral components (Lowenstam and Weiner 1989). Noteworthily, Ben Omar et al. (1994, 1995, 1998) and Gonzalez-Munoz et al. (1993, 1996) conducted a series of experiments on struvite formation with several soil inhabiting genera, like *Azotobacter*, *Bacillus*, *Myxococcus*, and *Pseudomonas*. One of their studies (Ben Omar et al. 1994) shows that the struvite precipitation would not occur until the autolysis of *M. Xanthus* cultures and the actual physical presence of the bacteria was necessary. Ben Omar et al. (1995, 1998) also found that dead cells, disrupted cells, and membrane fractions of this microorganism induce the struvite crystallization. Evidently, their observations lend support to our proposed biomineralization process of hazenite.

It has been well documented that ikaite, $CaCO_3 \cdot 6H_2O$, precipitates seasonally in Mono Lake (Shearman et al. 1989; Council and Bennett 1993; Bischoff et al. 1993). During the winter, cold water temperatures and high concentrations of PO_4^{3-} and organic carbon inhibit calcite precipitation, allowing the metastable ikaite to form. During the spring warming, however, ikaite decomposes to $CaCO_3$ and H_2O, occasionally leaving pseudomorphs of the primary precipitate. Yet, it is unclear whether and how the hazenite formation in Mono Lake may be affected by the seasonal weather changes or the diversion of tributary streams (Bischoff et al. 1991). Apparently, more systematic studies, including field observations, are needed to address these questions.

In environmental mineralogy, the precipitation of struvite from sewage has been a subject of considerable investigations because it may offer a potential route for dephosphorization of wastewater from industries and to recover phosphates for recycling in the form of fertilizer. At present, there are numerous research projects focusing on the controlled precipitation of struvite and its later utilization as a fertilizer (Booker et al. 1999; Doyle and Parsons 2002; Shu et al. 2006; Machnicha et al. 2008; Forrest et al. 2008) The discovery of hazenite and a better understanding of its formation process, especially in terms of the degree of biologically controlled vs. biologically induced mineralization (Lowenstam 1981; Mann 1983), will undoubtedly provide us with additional knowledge in this regard and facilitate future work on biomineralization of struvite-type phosphate materials.

ACKNOWLEDGMENTS

REFERENCES CITED

Angoni, K., Popp, J., and Kiefe, W. (1998) A vibrational spectroscopy study of "urinary sand." Spectroscopy Letters, 31, 1771–1782.
Banks, E., Chianelli, R., and Korenstein, R. (1975) Crystal chemistry of struvite analogs of the type $MgMPO_4 \cdot 6H_2O$ ($M^+ = K^+, Rb^+, Cs^+, Tl^+, NH_4^+$). Inorganic Chemistry, 14, 1634–1639.
Booker, N.A., Priestley, A.J., and Fraser, I.H. (1999) Struvite formation in waste-water treatment plants: Opportunities for nutrients recovery. Environmental Technology, 20, 777–782.
Ben Omar, N., Entrena, M., Gonzalez-Munoz, M.T., Arias, J.M., and Huetas, F. (1994) The effects of pH and phosphate on the production of struvite by *Myxococcus Xanthus*. Geomicrobiology Journal, 12, 81–90.
Ben Omar, N., Matinez-Canamero, M., Gonzalez-Munoz, M.T., Arias, J.M., and Huetas, F. (1995) *Myxocuccus xanthus*' killed cells as inducers of struvite crystallization: Its possible role in the biomineralization processes. Chemosphere, 30, 2387–2396.
Ben Omar, N., Gonzalez-Munoz, M.T., and Penalver, J.M.A. (1998) Struvite crystallization on *Myxocuccus* cells. Chemosphere, 36, 475–481.
Benson, L.V., Lund, S.P., Burdett, J.W., Kashgarian, M., Rose, T.P., Smoot, J.P., and Schwartz, M. (1998) Correlation of late-Pleistocene lake-level oscillations in Mono Lake, California, with North Atlantic climate events. Quaternary Research, 49, 1–10.
Bischoff, J.L., Herbst, D.B., and Rosenbauer, R.J. (1991) Gaylussite formation at Mono Lake, California. Geochimica et Cosmochimica Acta, 55, 1743–1747.
Bischoff, J.L., Stine, I.S., Rosenbauer, R.J., Fitzpatrick, J.A., and Stafford, Jr., T.W. (1993) Ikaite precipition by mixing of shoreline springs and lake water, Mono Lake, California, U.S.A. Geochimica et Cosmochimica Acta, 57, 3855–3865.
Blachnik, R., Wiest, T., Dulmer, A., and Reuter, H. (1997) The crystal structure of ammonium hexaaquanickel(II) phosphate. Zeitschrift für Kristallographie, 212, 20–23.
Budinoff, C.R. and Hollibaugh, J.T. (2007) Ecophysiology of a Mono Lake pico-cyanobacterium. Limnology and Oceanography, 52, 2486–2495.
Chen, L., Shen, Y., Xie, A., Huang, F., Zhang, W., and Liu, S. (2010) Seed-mediated synthesis of unusual struvite hierarchical superstructures using bacterium. Crystal Growth and Design, 10, 2073–2082.
Cohen, L.H. and Ribbe, P.H. (1966) Magnesium phosphate mineral replacement at Mono Lake, California. American Mineralogist, 51, 1755–1765.
Cooper, J.F. and Dunning, G.E. (1969) Struvite found at Mono Lake. Mineral Information Service, 22, 44–45.
Council, T.C. and Bennett, P.C. (1993) Geochemistry of ikaite formation at Mono Lake, California: Implications for the origin of tufa mounds. Geology, 21, 971–974.
Dickens, B. and Brown, W.E. (1972) The crystal structure of $CaKAsO_4 \cdot 8H_2O$. Acta Crystallographica B, 28, 3056–3065.
Downs, R.T., Bartelmehs, K.L., Gibbs, G.V., and Boisen, M.B. Jr. (1993) Interactive software for calculating and displaying X-ray or neutron powder diffractometer patterns of crystalline materials. American Mineralogist, 78, 1104–1107.
Doyle, J.D. and Parsons, S.A. (2002) Struvite formation, control, and recovery. Water Research, 36, 3925–3940.
El Bali, B., Essehli, R., Capitelli, F., and Lachkar, M. (2005) Reivestigation of $NH_4[Co(H_2O)_6]PO_4$ based on single-crystal data. Acta Crystallographica, 61, i52–i54.
Ferraris, G., Fuess, H., and Joswig, W. (1986) Neutron diffraction study of $Mg(NH_4)(PO_4) \cdot 6H_2O$ (struvite) and survey of water molecules donating short hydrogen bonds. Acta Crystallographica B, 42, 253–258.
Forrest, A.L., Fattah, K.P., Mavinic, D.S., and Koch, F.A. (2008) Optimizing struvite production for phosphate recovery in WWTP. Journal of Environmental Engineering, 134, 395–402.
Frost, R.L., Weier, M.L., Martens, W.N., Henry, D.A., and Mills, S.J. (2005) Raman spectroscopy of newberyite, hannayite, and struvite. Spectroschimica Acta A, 62, 181–188.
Garrels, R.M. and Mackenzie, F.T. (1967) Origin of the chemical composition of springs and lakes. In R.F. Gould, Ed., Equilibrium in Natural Water Systems, p. 222–242. American Chemical Society, Washington, D.C.
Gonzalez-Munoz, M.T., Arias, J.M., Montoya, E., and Rodriguez-Gallego, M. (1993) Struvite production by *Myxococcus coralloides D*. Chemosphere, 26, 1881–1887.
Gonzalez-Munoz, M.T., Ben Omar, N., Martinez-Canamero, M., Rodriguez-Gallego, M., Lopez-Galindo, A., and Arias, J.M. (1996) Struvite and calcite crystallization induced by cellular membranes of *Myxococcus xanthus*. Journal of Crystal Growth, 163, 434–439.
Graeser, S., Postl, W., Bojar, H.-P., Berlepsch, P., Armbruster, T., Raber, T., Ettinger, K., and Walter, F. (2008) Struvite-(K), $KMgPO_4 \cdot 6H_2O$, the potassium equivalent of struvite—a new mineral. European Journal of Mineralogy, 20, 629–633.
Grover, J.E., Rope, A.F., and Kaneshiro, E.S. (1997) The occurrence of biogenic calcian struvite, $(Mg, Ca)NH_4PO_4 \cdot 6H_2O$, as intracellular crystals in *Parame-*

cium. Journal of Eukaryotic Microbiology, 44, 366–373.

Haferburg, G., Kloess, G., Schmitz, W., and Kothe, E. (2008) "Ni-struvite"—a new biomineral formed by a nickel resistant streptomyces acidiscabies. Chemosphere, 72, 517–523.

Hollibaugh, J.T., Wong, P.S., Bano, N., Pak, S.K., Prager, E.M., and Orrego, C. (2001) Stratification of microbial assemblages in Mono Lake, California, and response to a mixing event. Hydrobiologia, 466, 45–60.

Jellison, R., Anderson, R.F., Melack, J.M., and Heil, D. (1996) Organic matter accumulation in sediments of hypersaline Mono Lake during a period of changing salinity. Limnology and Oceanography, 41, 1539–1544.

Jørgensen, N.O.G., Engel, P., Jellison, R., and Hollibaugh, J.T. (2008) Contribution of bacterial cell wall components to DOM in alkaline, hypersaline Mono Lake, California. Geomicrobiology Journal, 25, 38–55.

Koleva, V.G. (2007) Vibrational behavior of the phosphates ions in dittmarite-type compounds $M'M''PO4·H_2O$ (M'=K^+, NH_4^+; M''=Mn^{2+}, Co^{2+}, Ni^{2+}). Spectrochimica Acta, 66, 413–418.

Li, H-C., Ku, T-L., Stott, L.D., and Anderson, R.F. (1997) Stable isotope studies on Mono Lake (California). 1. $\delta^{18}O$ in lake sediments as proxy for climatic changes during the last 150 years. Limnology and Oceanography, 42, 230–238.

Lowenstam, H.A. (1981) Minerals formed by organisms. Science, 211, 1126–1131.

Lowenstam, H.A. and Weiner, S. (1989) Biomineralization, p. 324. Oxford University Press, New York.

Machnicha, A., Grubel, K., and Suschka, J. (2008) Enhanced biological phosphorus removal and recovery. Water Environment Research, 80, 617–623.

Mann, S. (1983) Mineralization in biological systems. Structure and Bonding, 54, 125–174.

Mathew, M. and Schroeder, L.W. (1979) Crystal structure of a struvite analogue, $MgKPO_4·6H_2O$. Acta Crystallographica B, 35, 11–13.

Mathew, M., Kingsbury, P., Takagi, S., and Brown, W.E. (1982) A new struvite-type compound, magnesium sodium phosphate heptahydrate. Acta Crystallographica, 38, 40–44.

Melack, J.B. (1983) Large, deep, salt lakes: A comparative limnological analysis. Hydrobiologia, 105, 223–230.

Mono Basin Ecosystem Study Committee (1987) The Mono basin ecosystem, 272 p. National Academy Press, Washington, D.C.

Oremland, R.S., Stolz, J.F., and Hollibaugh, J.T. (2004) The microbial arsenic cycle in Mono Lake, California. FEMS Microbiology Ecology, 48, 15–27.

Ribbe, P.H. and Cohen, L.H. (1966) Newberyite and monetite from Paoha Island, Mono Lake. Mineral Information Service, 19, 46.

Rivadeneyra, M.A., Perez-Garcia, I., and Ramos-Cormenzana, A. (1993) The effect of incubation temperature on struvite formation by bacteria. Folia Microbiology, 38, 5–9.

Robinson, H. (1889) On the formation of struvite by microorganisms. Proceedings of Cambridge Philosophical Society, 6, 360–362.

Shearman, D.J., McGugan, A., Stein, C., and Smith, A.J. (1989) Ikaite, $CaCO_3·6H_2O$, precursor of the thinolites in the Quaternary tufas and tufa mounds of the Lahontan and Mono Lake basins, western United States. GSA Bulletin, 101, 913–917.

Sheldrick, G.M. (2008) A short history of *SHELX.* Acta Crystallographica, 64, 112–122.

Shu, L., Schneider, P., Jegatheesan, V., and Johnsom, J. (2006) An economic evaluation of phosphorous recovery as struvite from digester supernatant. Bioresource Technology, 97, 2211–2216.

Stefov, V., Soptrajanov, B., Spirovski, F., Kuzmanovski, I., Lutz, H.D., and Engelen, B. (2004) Infrared and Raman spectra of magnesium ammonium phosphate hexahydrite (struvite) and its isomorphous analogues. I. Spectra of protiated and partially deuterated magnesium potassium phosphate hexahydrite. Journal of Molecular Structure, 689, 1–10.

Stefov, V., Soptrajanov, B., Kuzmanovski, I., Lutz, H.D., and Engelen, B. (2005) Infrared and Raman spectra of magnesium ammonium phosphate hexahydrite (struvite) and its isomorphous analogues. III. Spectra of protiated and partially deuterated magnesium ammonium phosphate hexahydrite. Journal of Molecular Structure, 752, 60–67.

Stine, S. (1994) Extreme and persistent drought in California and Patagonia during mediaeval time. Nature, 369, 546–549.

Touaiher, M., Bettach, M., Benkhouja, K., Zahir, M., Aranda, M.A.G., and Bruque, S. (2001) Synthesis and structure of $NH_4CoPO_4·6H_2O$. Annales de Chimie-science des Materiaux, 26, 49–54.

Trobajo, C., Salvado, M.A., Pertierra, P., Alfonso, B.F., Blanco, J.A., Khainakov, S.A., and Garcia, J.R. (2007) Synthesis, structure and magnetic characterization of two phosphate compounds related with the mineral struvite: $KNiPO_4·6H_2O$ and $NaNiPO_4·7H_2O$. Zeitschrift für Anorganische und Allgemeine Chemie, 633, 1932–1936.

Weil, M. (2008) The struvite-type compounds $M[Mg(H_2O)_6](XO_4)$, where M = Rb, Tl and X = P, As. Crystal Research Technology, 43, 1286–1291.

Walker, J. (1988) Paoha Island phosphates. Quarterly of San Bernardino County Museum Association, 35, 46–47.

Wiens, J.A., Patten, D.T., and Botkin, D.B. (1993) Assessing Ecological Impact Assessment: Lessons from Mono Lake, California. Ecological Applications, 3, 595–609.

Yang, H. and Sun, H.J. (2004) Crystal structure of a new phosphate compound, $Mg_2KNa(PO_4)_2·14H_2O$. Journal of Solid State Chemistry, 177, 2991–2997.